January 2009 *Volume 4 Issue 1*

Trade Science Inc.

Environmental Science

An Indian Journal

Current Research Papers

ESAIJ, 4(1), 2009 [14-25]

Salinity sources in coastal aquifers: Critical importance of sabkha deposits west of el bardaweil lake, North Sinai, Egypt

M.A.Gomaa*[1], T.Meixner[2], J.McIntosh[2]

[1]Department of Hydrogeochemistry, Desert Research Center, Matariya, (EGYPT)

[2]Department of Hydrology and Water Resources, University of Arizona, (U.S.A.)

E-mail : gomaa_57@hotmail.com

Received: 13th October, 2008 ; Accepted: 18th October, 2008

ABSTRACT

Salinization of aquifer waters is a pervasive problem worldwide. Increased salinity in groundwater can come from a diverse number of sources, among them dissolution of evaporites, evapoconcentration and seawater intrusion. Additionally, as groundwater becomes more saline geochemical evolution including exchange, precipitation and dissolution reactions can be facilitated and potentially alter water quality. In the current investigation we use a set of groundwater physical and chemical observations from a region close to El Bardaweil lagoon on the Mediterranean coast of Egypt. We investigate seawater intrusion and evaporite dissolution of sabkha deposits as the origin of the variability in total dissolved solids in the aquifer system. In addition, we investigate the impacts of increased salinity on mineral equilibrium reactions and geochemical evolution of the groundwater system. The dissolution of evaporites is identified as the source of salinization in this system with those evaporites likely originating from the sabkha deposits found in the area. We also hypothesize that dolomitization is occurring in this system through the addition of Mg from dissolution of Mg-rich evaporite minerals by meteoric waters, and a resulting shift in saturation indices for dolomite. The mechanism we propose differs from existing mechanisms in that it can occur in oxidizing environments and occurs after sabkha deposits are no longer in direct contact with seawater. The study also implies that development efforts by Egypt in the area to utilize Nile river water for agricultural purposes should proceed carefully as irrigated fields should be placed carefully to avoid dissolution of underlying evaporite deposits.

KEYWORDS

Africa;
Egypt;
Salinization;
Salt-water/fresh-water relations;
Coastal aquifers.

INTRODUCTION

Seawater intrusion is a pervasive problem in coastal aquifers around the world and can occur both due to static shifts in the groundwater table as well as dynamically through upcoming of saline waters during pumping[16]. Intrusion of seawater into freshwater aquifers can lead to degradation of water quality and risks to human infrastructure through increased corrosion. Additionally seawater intrusion can lead to a series of exchange, dissolution and precipitation reactions that can further alter aquifer water quality[1].

While seawater intrusion can be induced by human activities it is also well known to occur due to natural interactions between land and sea in coastal sabkha environments[13]. In these environments it is well established that dolomitization can occur[4] although it need not occur in a given sabkha environment[6]. Since it is still not certain how the hydrology of sabkhas function and what role they may play in dolomite formation in modern times (and by inference in geologic time)[6,13] additional studies on the hydrologic and geochemical processes in coastal environments where sabkhas are present are necessary.

Due to their geographic position sabkhas represent the terminus of terrestrial aquifer systems. As fresh groundwaters (Cl < 200 mmol/L) migrate through sabkha deposits, they dissolve solutes from evaporite minerals. It has been shown that direct rainfall and subsequent infiltration and recharge can also be a major source of water in sabkha dominated regions. It is likely that until mineral dissolution and evapoconcentration occur that local recharge results in a freshwater lens overlying more brackish waters. In either of these situations, as fresh and saline waters mix and fresh water inputs interact with sabkha deposits the chemistry of the system will continue to evolve and be subject to a series of dissolution and precipitation reactions. Given that sabkha deposits are one of several places where dolomitization is currently occurring investigations of fresh/saline water interaction should prove a productive avenue for research into the possible controls on dolomitization.

While much research has been done on sabkha systems and in parallel much work has been done on seawater intrusion there are few studies that focus on understanding the salinization of groundwaters in near coastal environments where both sabkha and seawater intrusion processes are occurring. Here, we investigate the geochemical evolution of groundwaters in a near coastal environment on the north coast of Egypt between the Nile Delta and the edge of El Bardaweil Lake (a coastal lagoon). The land surface above the aquifer system varies between sand dunes and the surface expression of sabkha deposits. These surface properties allow for both local recharge and more regionally driven hydraulic gradients. This setting is ideal for investigating the following questions :

(1) Are salinity differences in this coastal aquifer caused by evaporite dissolution or seawater intrusion ?

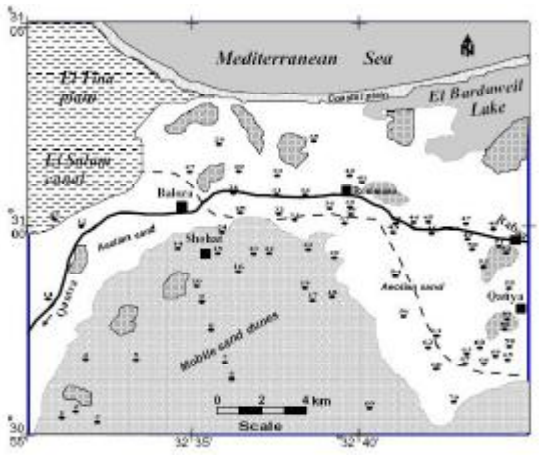

Figure 1: Map of Region between El Bardaweil and El Tina Plain. Crosschecked areas are surface expressions of Sabkhas. Coastal plain, Aeolian sand and mobile sand dunes are all areas dominated by sand deposits of different types and geomorphic mobility

(2) How does chemical evolution of the system affect the diagenetic reactions that are occurring ?

(3) What insight can conditions observed here tell us about mineral precipitation conditions in other hydrogeologic systems ?

Site description

The investigated area is located immediately to the west of El Bardaweil Lake, North Sinai, Egypt. It lies roughly within a rectangle defined by 30° 55' N and 31° 5' N and 32° 30' E and 32° 45' E. Aeolian sand, silt, clay, shell fragments related to the Quaternary period cover the surface of the study area. At El Tina plain, the thickness of the Quaternary deposits is about 455 m. These deposits are sand, silt and clay, where the main source of deposition is the Nile River (Pelusium) with normal regression of the Mediterranean Sea. In the subsurface, the geologic succession is represented by Pre-Miocene calcareous deposits, Miocene and Pliocene clay, Lower Pleistocene (Kurkar Formation) and Upper Pleistocene (gravelly deposits) (Figure 1).

Close to the Mediterranean Sea, marshes and ponds comprise large fractions of the surface of the study area. Most of these lentic and near lentic environments are connected to El Bardaweil lake (a coastal sabkha). To the south, depressions between aeolian dunes upland deposits are covered with sabkha deposits due to the evaporation of seawater/groundwater or both (continental sabkha) during the recent geologic past.

Current Research Paper

METHODS

Sampling

In the investigated area, 70 groundwater samples were collected during March (2007). The depths to the groundwater surface were measured using an electric line sounder (Richter measuring tool, 100-200 m) and well locations were estimated using a field GPS instrument (Magellan colour trak). Samples were collected using a peristaltic pump at the surface. Samples for analyses were immediately filtered through 0.45 micrometer cellulose membrane filters. The performed chemical analyses included the determination of E.C, pH, T.D.S, Ca, Mg, Na, K, Alkalinity, SO_4, Cl, and Br. These groundwater sample analyses were carried out at the central lab of Desert Research Center according to the methods adopted by Fishman and Friedman[12], and Rainwater and Thatcher[12]. The instruments used were a pH meter, E.C meter, Flame photometer, Spectrophotometer, Ion analyzer (Ion Selective Electrode) and ICP.

These data were subsequently used in graphical analyses to understand geochemical interactions within the aquifer system. These graphs included mixing plots as well as graphs of ion ratios. Comparisons were made to seawater composition and the population of samples was divided according to high and low chloride concentrations to aid in the visualization of the processes occurring in the aquifer system (TABLES 1-6, inclusive).

TABLE 1: Longitudes and latitudes and some hydrogeological data

Well no.	Lat.	Long.	D.T.W (m)	W.L (m)	Well No.	Lat.	Long.	D.T.W (m)	W.L (m)
1	30.9279418726	32.5099574182	0.5	7.96	36	31.0168781623	32.6370654319	6	
2	30.9326679584	32.5136189511	1.44	7.56	37	31.022033903	32.6279115451	1.35	-1
3	30.9396854779	32.50760356	3		38	31.0241821184	32.633403899	5.5	
4	30.9359618906	32.5455267274	2.6	6.6	39	31.0238956817	32.6378500149	9	
5	30.9525748	32.5452651816	2.4	6.12	40	31.0237524634	32.6572039174	0.85	8.45
6	30.9845116536	32.5334959453	3		41	31.0277624873	32.652757747	4.3	2.7
7	30.9822202199	32.5434344151	3.69	0.45	42	31.0390764375	32.6279115451	13.5	
8	30.9774941341	32.5633114093	4.5	1.18	43	31.0382171275	32.6226807916	3.71	2.29
9	30.9746298569	32.5803114537	5	1.04	44	31.0449482402	32.6284346368	7	
10	30.9729112667	32.5897268318	4		45	31.0499607328	32.6286961827	7	1.17
11	30.9235022236	32.5818806743	2.52	7.4	46	31.0511064496	32.6221576999	3.5	-2.92
12	30.9346729554	32.6263423245	2.1	3.2	47	31.0624204297	32.6276499992	11	1.19
13	30.9255072206	32.6305269491	1.63	0.37	48	31.0714429462	32.6247731039	8	
14	30.9664666206	32.6130038131			49	31.0629932732	32.6187576583	6	1.89
15	30.9797855678	32.6098653719	6.12	5.35	50	31.0645686451	32.6124807214	8	
16	30.9868030873	32.5991422645	3.7	3.96	51	31.0733047249	32.6143115424	7	1.78
17	31.0114360147	32.5808344909	3	3.92	52	31.0758825953	32.6101269177		
18	31.0177374424	32.583188349	2.5		53	31.0680057956	32.6017576685	2.5	3.37
19	31.0088581443	32.5886807029	2.2	3.76	54	31.0389332192	32.5962653146	9.95	-0.3
20	31.0185967226	32.6072499679	2		55	31.0767418755	32.5884191571	3	3.51
21	31.0100038611	32.61221923	0.5	3.14	56	31.0415110896	32.5716806586		
22	30.9969713207	32.6098653719	5.35		57	31.076169032	32.5698498921	3	1.17
23	30.9916723914	32.609603826	4.85	3.82	58	31.0753097219	32.563834501	6	
24	30.9812177214	32.6229422829	7.82	3.54	59	31.0768850938	32.5536344308		
25	30.9873759607	32.6344500279	3.75		60	31.0668600788	32.5528498478	8.7	0.96
26	30.985084527	32.64648081	3.6	0.41	61	31.0525386031	32.5596498764	6	1.94
27	30.970619833	32.6595577756	6.8	-2.72	62	31.0498175144	32.5528498478	5.85	2.65
28	30.9802152229	32.6760347282	0.98	1	63	31.0627068365	32.548926769	5	2.6
29	30.9869463057	32.6598193215			64	31.072159008	32.5476190397	6	2.28
30	30.9996924094	32.6572039174	3		65	31.0763122204	32.5452651816	3.1	3.85
31	30.9995491911	32.645696227	7	0.68	66	31.0682922024	32.5426498321	3	
32	31.0002652529	32.6336653903	2.05	3.57	67	31.062133993	32.5429113234	8	2.71
33	31.0052777754	32.6300038574	1.8	3.3	68	31.0525386031	32.5395113364	5	
34	31.0088581443	32.6454346811	3.5	2.55	69	31.0301971095	32.5157112634	5.3	1.71
35	31.0118656398	32.6781270405	2.75	3.85	70	31.0582671874	32.5196343967	6	6.65

TABLE 2 : The hydrochemical analyses data of the groundwater samples (mg/l)

Well no.	pH	E.C	TDS (mg/l)	Ca	Mg	Na	K	CO_3	HCO_3	SO_4	Cl	Alkalinity as $CaCO_3$
1	8.4	6510	4166	224	145.8	950	23	4.35	57.49	512.5	1944.25	54.41016
2	7.7	5450	3488	187.1	95.54	1000	20	Nil	110.71	400	1730.8	90.81757
3	8.3	8260	5286	400	170.1	1100	39	2.18	61.92	733.33	2398.75	54.42751
4	7.8	10859	6950	394	287.28	1800	56	Nil	224.78	800	3500.9	184.3914
5	7.1	4518	2892	150.6	90.36	810	9		104	380	1400.2	85.31323
6	8.3	3760	2406	152	29.16	520	24	4.35	70.77	80	1111	65.304
7	8	2357	1509	94.57	43.09	420	11		104	160	728.7	85.31323
8	8.3	6110	3910	280	140.94	825	19.5		66.34	350	1893.75	54.42
9	8.4	6250	4000	280	121.5	860	19.5		66.35	400	1893.75	54.4282
10	8.3	6420	4018	256	126.36	850	16	4.35	66.35	425	1792.75	61.67819
11	7.8	38906	24900	510.2	1549.7	4300	31	41.09	20.89	538.8	11621.7	85.61974
12	8.8	2700	1728	48	58.32	420	37	4.35	112.79	280	662.4	99.77383
13	7.4	6701	4289	98.3	154.85	1250	15	7.74	106.64	520	2192.89	100.3789
14	8.2	13520	8652	608	306.18	1750	33		53.08	400	4469.25	43.54256
15	7.9	23062	14760	612.24	619.9	2760	23	16.43	45.95	2072	5544	65.07699
16	8.3	4706	3012	114.28	71.82	940	9		132.85	220	1591	108.9794
17	8.1	9500	6080	392	193.18	1700	19.5		35.38	1000	3156.25	29.0229
18	8.2	11910	7622	464	222.34	1800	30.5	13.05	26.34	900	3512	43.35719
19	7.9	11000	7041	354.67	257.35	1800	36		117.42	875	3659.47	96.32192
20	8	23000	14720	1080	279.45	3700	32	4.35	79.61	1900	6767	72.55563
21	8.1	15860	10150	702	388.8	2000	32		84.04	1250	4710	68.93965
22	7.1	5580	3571	257.14	4.96	925	13	12.32	142.05	344.05	1633.5	137.0597
23	7.8	10615	6794	384.2	245.38	1750	16.5		106.01	850	3495	86.96207
24	7.7	7662	4904	330.2	224.43	1200	16	19.8	127.45	500	2550.2	137.5497
25	8.3	15020	9612	284	228.42	2700	43.5	18.87	77.4	420	5100.5	94.9427
26	7.9	10479	6707	177.33	149.62	2200	35	13.2	201.3	400	3631.2	187.1303
27	7.1	55100	35264	2060	952.1	8460	40	41.12	170.36	1400	18500	208.2829
28	7.6	115312	73800	612.24	2355.6	19000	300	61.64	29.14	680	35815	126.6373
29	8.2	22900	14656	78	19.44	5100	58		207.83	860	7575	170.487
30	8.9	1338	856	30	12.44	225	10	20.4	190.11	80	234.15	189.9509
31	8	2512	1608	157.63	95.76	280	6		134.39	443.3	544	110.2427
32	7.4	21229	13587	784.28	571.71	3500	81		221.43	1300	7240.2	181.6433
33	7.9	5734	3670	295.26	136.46	850	23	6.6	140.91	600	1688.2	126.5912
34	8.7	4800	3072	418	98.41	460	18	4.35	90.67	860	1010	81.62836
35	8	50220	32141	2064.1	972.77	8486.7	39.93	45.52	168.28	1450	18563	213.91
36	8.3	10320	6604	770	256.36	1000	32		97.31	1150	2903.75	79.82529
37	8.1	9942	6362	43.86	150.17	1638.7	43	16.55	101	1260	2722.5	110.4356
38	8.2	10880	6963	533.12	166.7	1600	49		44.23	400	3480	36.28273
39	8.6	3600	2304	156.8	85.73	510	17		99.52	120	1200	81.6382
40	7.3	116250	74400	1632.6	2107.6	18000	198		125.34	5923.5	34155	102.8188
41	8.1	2140	1370	47.28	31.12	410	8	16.5	254.98	400	330.35	236.665
42	8.6	3700	2368	156.8	83.35	440	16	2.17	90.67	100	1058	77.99503
43	8.1	2320	1485	128.07	71.82	320	8	16.5	144.25	160	709.29	145.8311
44	8.7	2220	1420	86.24	54.77	320	18	4.35	181.34	90	620	156.0067
45	8.8	1000	640	48	25.1	140	7	2.17	119.42	70	260	101.5792
46	8.8	5770	3692	196	142.88	840	38.5	4.35	103.94	280	1852	92.514
47	8.5	4010	2566	196	88.11	550	13.5		101.73	120	1287.75	83.4511
48	8.8	5580	3571	19.6	135.74	900	45		154.81	110	1730	126.9937
49	8.8	2670	1708	100	59.54	420	13.5		165.86	80	812.4	136.0582
50	8.8	1547	990	141.12	26.2	150	7.5	8.7	136.11	100	388	126.1537
51	8.2	10800	6912	266.56	285.77	1600	45		163.65	260	3612	134.2453
52	8.5	6800	4352	462.56	195.27	740	29		137.11	40	2498	112.474
53	7.7	10509	6726	450.19	271.3	1650	17		134.2	640	3631.1	110.0869
54	7.5	6055	3875	400	83.26	916.98	15	16.55	101	365	1979	110.4356

TABLE 3 : The hydrochemical analyses data of the groundwater samples (mmol/L)

Well no.	Ca (mmol/L)	Mg (mmol/L)	Na (mmol/L)	K (mmol/L0	CO_3 (mmol/L)	HCO_3 (mmol/L)	SO_4 (mmol/L)	Cl (mmol/L)
1	5.5888	5.995296	41.306	0.58834	0.072493	0.942261	5.335125	54.82785
2	4.668145	3.928605	43.48	0.5116		1.814537	4.164	48.80856
3	9.98	6.994512	47.828	0.99762	0.03633	1.014869	7.633965	67.64475
4	9.8303	11.81295	78.264	1.43248		3.684144	8.328	98.72538
5	3.75747	3.715603	35.2188	0.23022		1.70456	3.9558	39.48564
6	3.7924	1.199059	22.6096	0.61392	0.072493	1.15992	0.8328	31.3302
7	2.359522	1.771861	18.2616	0.28138		1.70456	1.6656	20.54934
8	6.986	5.795453	35.871	0.49881		1.087313	3.6435	53.40375
9	6.986	4.99608	37.3928	0.49881		1.087477	4.164	53.40375
10	6.3872	5.195923	36.958	0.40928	0.072493	1.087477	4.42425	50.55555
11	12.72949	63.72366	186.964	0.79298	0.684765	0.342387	5.608908	327.7319
12	1.1976	2.398118	18.2616	0.94646	0.072493	1.848628	2.9148	18.67968
13	2.452585	6.367432	54.35	0.3837	0.128987	1.74783	5.4132	61.8395
14	15.1696	12.59012	76.09	0.84414		0.869981	4.164	126.0329
15	15.27539	25.49029	120.0048	0.58834	0.273806	0.753121	21.56952	156.3408
16	2.851286	2.953238	40.8712	0.23022		2.177412	2.2902	44.8662
17	9.7804	7.943562	73.916	0.49881		0.579878	10.41	89.00625
18	11.5768	9.142621	78.264	0.78019	0.217478	0.431713	9.369	99.0384
19	8.849017	10.58223	78.264	0.92088		1.924514	9.10875	103.1971
20	26.946	11.49098	160.876	0.81856	0.072493	1.304808	19.779	190.8294
21	17.5149	15.98746	86.96	0.81856		1.377416	13.0125	132.822
22	6.415643	0.203955	40.219	0.33254	0.205313	2.3282	3.581561	46.0647
23	9.58579	10.09003	76.09	0.42207		1.737504	8.8485	98.559
24	8.23849	9.228562	52.176	0.40928	0.329967	2.088906	5.205	71.91564
25	7.0858	9.39263	117.396	1.11273	0.314469	1.268586	4.3722	143.8341
26	4.424384	6.152374	95.656	0.8953	0.219978	3.299307	4.164	102.3998
27	51.397	39.15035	367.8408	1.0232	0.685265	2.7922	14.574	521.7
28	15.27539	96.86227	826.12	7.674	1.027231	0.477605	7.0788	1009.983
29	1.9461	0.799373	221.748	1.48364		3.406334	8.9526	213.615
30	0.7485	0.511533	9.783	0.2558	0.339966	3.115903	0.8328	6.60303
31	3.932869	3.937651	12.1744	0.15348		2.202652	4.614753	15.3408
32	19.56779	23.50872	152.18	2.07198		3.629238	13.533	204.1736
33	7.366737	5.611235	36.958	0.58834	0.109989	2.309515	6.246	47.60724
34	10.4291	4.046619	20.0008	0.46044	0.072493	1.486081	8.9526	28.482
35	51.4993	40.0003	369.0017	1.021409	0.758591	2.758109	15.0945	523.4766
36	19.2115	10.54152	43.48	0.81856		1.594911	11.9715	81.88575
37	1.094307	6.17499	71.25068	1.09994	0.275806	1.65539	13.1166	76.7745
38	13.30134	6.854704	69.568	1.25342		0.72493	4.164	98.136
39	3.91216	3.525218	22.1748	0.43486		1.631133	1.2492	33.84
40	40.73337	86.66451	782.64	5.06484		2.054323	61.66364	963.171
41	1.179636	1.279654	17.8268	0.20464	0.274973	4.179122	4.164	9.31587
42	3.91216	3.427352	19.1312	0.40928	0.036163	1.486081	1.041	29.8356
43	3.195347	2.953238	13.9136	0.20464	0.274973	2.364258	1.6656	20.00198
44	2.151688	2.252142	13.9136	0.46044	0.072493	2.972163	0.9369	17.484
45	1.1976	1.032112	6.0872	0.17906	0.036163	1.957294	0.7287	7.332
46	4.8902	5.875226	36.5232	0.98483	0.072493	1.703577	2.9148	52.2264
47	4.8902	3.623083	23.914	0.34533		1.667355	1.2492	36.31455
48	0.48902	5.581629	39.132	1.1511		2.537336	1.1451	48.786
49	2.495	2.448285	18.2616	0.34533		2.718445	0.8328	22.90968

TABLE 4: Iodide and Bromide concentrations (mg/l) or (ppm)

No.	I	Br	No.	I	Br	No.	I	Br
1	0.04	21.4	25	0.065	20.9	49	-	-
2	-	-	26	-	-	50	-	-
3	0.038	20.8	27	0.07	25.1	51	-	-
4	-	-	28	0.084	33.7	52	0.07	56.3
5	-	-	29	0.071	30.9	53	-	-
6	0.035	20.7	30	0.075	32.8	54	0.06	29.3
7	-	-	31	-	-	55	0.055	31.2
8	0.042	22.7	32	-	-	56	-	-
9	0.045	28.4	33	-	-	57	0.063	32.3
10	0.044	25.4	34	0.065	20.9	58	0.058	28.2
11	0.056	23.8	35	0.09	35.8	59	0.052	24.3
12	0.068	28.9	36	0.064	29.5	60	0.072	32.4
13	-	-	37	0.059	32.9	61	0.068	29.3
14	0.058	30.7	38	0.055	34.4	62	0.064	17.1
15	0.055	28.2	39	0.063	40.1	63	0.06	23.3
16	-	-	40	0.07	39.1	64	0.039	12.9
17	0.05	48.1	41	-	-	65	0.053	22.9
18	0.05	44.2	42	-	-	66	0.055	18.3
19	-	-	43	0.05	15.7	67	0.058	20.9
20	0.049	55.4	44	-	-	68	0.061	25.3
21	0.057	48.3	45	-	-	69	0.028	17.8
22	0.056	50.9	46	0.063	19.4	70	-	-
23	0.058	54.5	47	0.058	20.7	-	-	-
24	-	-	48	0.062	21.3	-	-	-

Equilibrium modeling

Results of these analyses were used within PHREEQC[11] to calculate saturation indices of major minerals that might be either dissolving or precipitating within the aquifer system of El Bardaweil. Both the PHREEQ and PITZER databases were used for these calculations. Groundwater temperatures were not measured during sample collection, and were assumed to be approximately equal to the mean annual temperature (21.5^{0}C) as observed at Port Said on the Mediterranean coast some 30 km from the study basin. There is no known geothermal activity in the basin. Groundwater temperatures likely do not depart from mean annual temperature by more than 5^{0}C, which should have minimal effect on the equilibrium constants that are part of the saturation index calculations used in our analysis. After initial results, the PHREEQ database was discarded in favor of the PITZER database given generally high salinities within the aquifer system in the particular area of interest (ionic strengths between 0.04-1.22 mol/l). The saturation state for dolomite was cal-

TABLE 5 : Cl/Br and I/Br ratios

Well no.	Lat	Long	Cl/Br	I/Br	CI/CO_3 and HCO_3
1	30.9279418726	32.5099574182	204.712844425234	0.00117686646570395	50.4342176516381
2	30.9326679584	32.5136189511			26.8986318217061
3	30.9396854779	32.50760356	259.853404543269	0.00115027380998852	62.2041967780415
4	30.9359618906	32.5455267274			26.7973712863899
5	30.9525748	32.5452651816			23.1647111277984
6	30.9845116536	32.5334959453	120.934572	0.00106458089711625	24.0119505634418
7	30.9822202199	32.5434344151			12.0555099263153
8	30.9774941341	32.5633114093	187.976494823789	0.00116494226803382	49.1153602009211
9	30.9746298569	32.5803114537	150.248818045775	0.000997642963444458	49.1079577351787
10	30.9729112667	32.5897268318	159.035021893701	0.00109068648042012	41.0243104229666
11	30.9235022236	32.5818806743	1100.27048192773	0.0014814671980038	191.579462274771
12	30.9346729554	32.6263423245	51.6451138878893	0.0014814671980038	9.37037289154847
13	30.9255072206	32.6305269491			30.8338520549453
14	30.9664666206	32.6130038131	328.022044973941	0.00118951682184995	144.868475318777
15	30.9797855678	32.6098653719	442.976688	0.0012279892111113	120.240001938104
16	30.9868030873	32.5991422645			20.6052921094612
17	31.0114360147	32.5808344909	147.853999740125	0.000654494344232446	153.491284893966
18	31.0177374424	32.583188349	179.035435221719	0.000712243845194133	114.326400682645
19	31.0088581443	32.5886807029			53.6224027076345
20	31.0185967226	32.6072499679	275.22835232491	0.00055688726350955	131.637086111537
21	31.0100038611	32.61221923	219.725537142857	0.000743034013905631	96.4284127463055
22	30.9969713207	32.6098653719	72.311623956778	0.000692709613211991	16.8214163056511
23	30.9916723914	32.609603826	144.496536110092	0.000670058099647589	56.7244769925409
24	30.9812177214	32.6229422829			26.1678368981228
25	30.9873759607	32.6344500279	549.88671091866	0.00195815939449066	75.8235953687933
26	30.985084527	32.64648081			27.3879332963703
27	30.970619833	32.6595577756	1660.75192828685	0.00175592227651844	125.363559127433
28	30.9802152229	32.6760347282	2394.64871412463	0.00156938809996248	399.168592918092

Countinue next page

Current Research Paper

TABLE 5 : Cl/Br and I/Br ratios

Well no.	Lat	Long	Cl/Br	I/Br	CI/CO_3 and HCO_3
29	30.9869463057	32.6598193215	552.371059223301	0.00144670785436131	62.7111195829111
30	30.9996924094	32.6572039174	16.0852226542683	0.00143968801635277	1.73982666472633
31	30.9995491911	32.645696227			6.96469496930541
32	31.0002652529	32.6336653903	784.321258811538	0.00211892543945255	56.2579959973413
33	31.0052777754	32.6300038574			18.8223366124686
34	31.0088581443	32.6454346811	108.888457607656	0.00195815939449066	17.4635882468248
35	31.0118656398	32.6781270405	1168.34713109497	0.00158285252300685	122.481460368094
36	31.0168781623	32.6370654319	221.79102361017	0.00136596297578655	51.3418962777168
37	31.022033903	32.6279115451	186.457024285714	0.00112911215774909	34.7946186389788
38	31.0241821184	32.633403899	227.943682325581	0.00100666557422496	135.373126525234
39	31.0238956817	32.6378500149	67.4285206982544	0.00098918414530054	20.7463181416007
40	31.0237524634	32.6572039174	1968.26826705882	0.00112720330282898	468.850900048512
41	31.0277624873	32.652757747			1.97012324354485
42	31.0390764375	32.6279115451			19.1457294074607
43	31.0382171275	32.6226807916	101.796053895287	0.00200517057054654	6.86478584415217
44	31.0449482402	32.6284346368			5.60920798137296
45	31.0499607328	32.6286961827			3.6126149439276
46	31.0511064496	32.6221576999	215.10277385567	0.00204465382611091	28.2544401426593
47	31.0624204297	32.6276499992	140.174163	0.00176416262950694	21.7797388881922
48	31.0714429462	32.6247731039	183.009341408451	0.00183270707358686	19.2272532777391
49	31.0629932732	32.6187576583			8.42749315472733
50	31.0645686451	32.6124807214			4.34095233629098
51	31.0733047249	32.6143115424			37.9753588766932
52	31.0758825953	32.6101269177	99.9748583872114	0.000782835686334155	31.346817679645
53	31.0680057956	32.6017576685			46.553876314026
54	31.0389332192	32.5962653146	152.189584832765	0.00128933152044699	25.2923967994634
55	31.0767418755	32.5884191571	322.765281432692	0.00110991332542752	75.5885055531376
56	31.0415110896	32.5716806586			55.9981596135188
57	31.076169032	32.5698498921	246.600330464396	0.00122805833518736	76.3997520248
58	31.0753097219	32.563834501	332.8917075	0.00129497044080828	72.0286232978701
59	31.0768850938	32.5536344308	194.330048777778	0.00134734259571539	40.7682020420058
60	31.0668600788	32.5528498478	110.9718927	0.00139916346478136	65.7132526313053
61	31.0525386031	32.5596498764	194.1782221843	0.00146124238983992	98.223317378223
62	31.0498175144	32.5528498478	331.054452126316	0.00235648583542124	37.5880670903076
63	31.0627068365	32.548926769	241.415422702146	0.00162134822099128	29.0963912338947
64	31.072159008	32.5476190397	290.632561702326	0.0019035130858072	20.3175764734818
65	31.0763122204	32.5452651816	266.649373100437	0.00145720736397535	70.2746220263151
66	31.0682922024	32.5426498321	310.897372131148	0.00189231124335184	54.580261652585
67	31.062133993	32.5429113234	206.359798719617	0.00174728069046859	59.5873915556594
68	31.0525386031	32.5395113364	173.156319	0.00151806470783591	44.4899766229802
69	31.0301971095	32.5157112634	198.322779094382	0.000990419081811527	21.714221175427
70	31.0582671874	32.5196343967			24.4797733601971

culated using the K equilibrium value for moderately ordered sedimentary dolomite from Hyeong and Capuano[7] (Log Ksp = -8.42 at 21.5^{0}C versus -8.54 for PHREEQ database). To compare the ion activity product (IAP) for dolomite on the same molar basis as calcite, the square root was taken of the IAP dolomite from PHREEQ. Saturation indices reported by PHREEQ vary from negative values (undersaturated) to positive values (super-saturated) with a value of zero (±0.25 for calcite and dolomite[14]) indicating equilibrium between the aqueous solution and the particular mineral phase.

Reaction path modeling

After graphical analysis and equilibrium modeling with the compositions for the sample analyses for El Bardaweil system some simple reaction path modeling was conducted for the system to determine what minerals might be either dissolving or precipitating to explain the variability in solutions observed in the aquifer system. Two end member compositions were defined as the dilute waters (Cl < 50 mmol L-1) and the saline

TABLE 6: Values of saturation Indices of minerals

Well no.	Calcite	Gypsum	Dolomite	Halite	Aragonite
1	0.57	-0.9	1.45	-4.42	0.38
2	0.16	-1.06	0.38	-4.45	0.01
3	0.73	-0.62	1.45	-4.29	0.59
4	0.74	-0.69	1.71	-3.94	0.60
5	-0.53	-1.13	-0.93	-4.62	-0.67
6	0.62	-1.65	0.87	-4.89	0.47
7	0.26	-1.52	0.54	-5.15	0.12
8	0.66	-0.99	1.37	-4.50	0.51
9	0.74	-0.92	1.48	-4.48	0.60
10	0.67	-0.93	1.40	-4.51	0.53
11	0.33	-1.14	1.53	-3.11	0.18
12	0.74	-1.59	1.92	-5.19	0.60
13	-0.41	-1.28	-0.26	-4.26	-0.55
14	0.66	-0.84	1.39	-3.85	0.52
15	-1.22	-1.93	-0.38	-3.59	-1.36
16	0.64	-1.46	1.43	-4.50	0.49
17	0.23	-0.56	0.50	-4.00	-4.00
18	0.55	-0.56	1.14	-3.94	0.41
19	0.51	-0.69	1.25	-3.92	0.37
20	0.82	-0.10	1.41	-3.39	0.67
21	0.77	-0.36	1.65	-3.79	0.63
22	-0.10	-0.94	-1.56	-4.50	-0.24
23	0.41	-0.66	0.99	-3.95	0.27
24	0.51	-0.87	1.21	-4.23	0.37
25	0.77	-1.12	1.82	-3.61	0.63
26	0.55	-1.25	1.39	-3.83	0.41
27	0.58	-0.22	1.23	-2.63	0.44
28	0.30	-1.20	1.61	-1.98	0.15
29	0.33	-1.43	0.43	-3.19	0.19
30	1.03	-2.14	2.03	-5.88	0.88
31	0.53	-0.96	1.19	-5.46	0.39
32	0.53	-0.42	1.28	-3.38	0.38
33	0.66	-0.75	1.33	-4.54	0.51
34	1.30	-0.43	2.32	-5.02	1.16
35	1.43	-0.21	2.94	-2.63	1.29
36	1.10	-0.27	2.07	-4.27	0.95
37	-0.12	-1.34	0.63	-4.07	-0.27
38	0.57	-0.81	1.00	-3.99	0.43
39	0.95	-1.54	1.99	-4.87	0.81
40	0.30	0.13	1.12	-2.02	0.15
41	0.47	-1.42	1.10	-5.50	0.32
42	0.32	-1.60	1.97	-4.99	0.80
43	0.71	-1.43	1.52	-5.28	0.57
44	1.14	-1.79	2.43	-5.33	0.99
45	0.89	-1.99	1.85	-6.03	0.74
46	1.16	-1.21	2.54	-4.50	1.01
47	0.95	-1.47	1.91	-4.81	0.81
48	0.38	-2.53	1.96	-4.48	0.23
49	1.20	-1.82	2.53	-5.11	1.05
50	1.36	-1.48	2.35	-5.85	1.22
51	0.86	-1.29	2.11	-3.97	0.71
52	1.32	-1.79	2.63	-4.44	1.17
53	0.49	-0.72	1.13	-3.96	0.35
54	0.36	-0.83	0.38	-4.44	0.21

to be countinue in right column

TABLE 6: Values of saturation Indices of minerals

Well no.	Calcite	Gypsum	Dolomite	Halite	Aragonite
55	1.03	-0.71	2.24	-3.82	0.89
56	0.59	-0.77	1.27	-4.11	0.44
57	1.17	-0.57	2.39	-4.05	1.03
58	1.05	-0.81	2.18	-3.96	0.91
59	0.90	-0.73	1.79	-4.40	0.76
60	-0.18	-0.83	-1.37	-4.59	-0.32
61	0.94	-0.67	1.91	-4.25	0.80
62	0.69	-1.13	1.64	-4.31	0.54
63	0.30	-0.72	0.71	-4.26	0.16
64	0.76	-1.27	1.53	-4.68	0.61
65	0.71	-0.66	1.40	-4.25	0.56
66	1.29	-1.09	2.66	-4.34	1.14
67	0.98	-0.92	1.96	-4.46	0.83
68	0.72	-0.92	1.44	-4.45	0.57
69	0.36	-0.86	0.83	-4.57	0.21
70	0.40	-0.71	0.93	-4.37	0.25

waters (Cl >200 mmo L-1). The median chemical composition of these two end members were used as initial (dilute waters) and final (saline waters) for the reaction path modeling. Ten other combinations of dilute and saline waters were used for reaction path modeling, while these results are not reported they yielded similar interpretations. Again the PITZER database was used within PHREEQC and after initial broad inclusion of phases the input file was limited to the following mineral phasesthat could potentially be dissolving or precipitating: halite (NaCl), gypsum ($CaSO_4.2H_2O$), carbon dioxide (CO_2), calcite ($CaCO_3$), dolomite ($CaMg(CO_3)_2$), epsomite ($MgSO_4$), mirabilite ($Na_2SO_4.10H_2O$), and leonite ($K_2Mg(SO_4)_2.4H_2O$). Available mineral phases were limited to these to ensure a reasonable number of phases and that all major anions and cations in available chemical analyses were utilized. Several initial runs were completed with a much longer list of minerals (30), those selected were a combination of minerals closest to saturation and including all possible dissolved chemical species.

RESULTS

Hydraulic heads in the region of El Bardaweil Lake indicate a complex inland flow regime dominated by upland recharge and discharge into the sabkhas in the study area. There is also a more coastal flow regime running parallel to the Mediterranean from east to west (Figure 2). In this aquifer system chloride concentrations serve as a good surrogate for total dissolved solids. Comparisons of chloride concentrations to ground-

water elevations indicate no coherent relationship between the two environmental variables (Figure 3). Groundwaters are dominated by sodium (Na^+) and chloride (Cl^-). Notably, samples with the highest Cl concentrations have the lowest Br/Cl ratios, which are significantly less than seawater (Figure 4).

Mixing diagrams of the aqueous chemical data indicate that seawater intrusion and mixing with freshwaters is unlikely to be the source of increased salinity in the aquifers of the el Bardaweil region (Figure 5). The

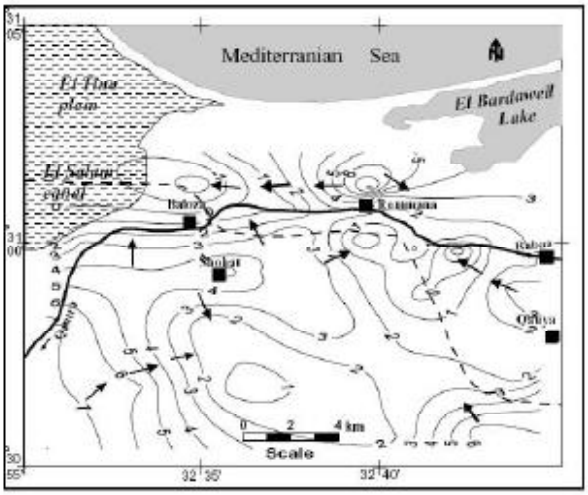

Figure 2: Map of water table elevation for region. Arrows utilize water table elevation derived from all well locations in figure 1 to indicate likely direction of regional groundwater flow

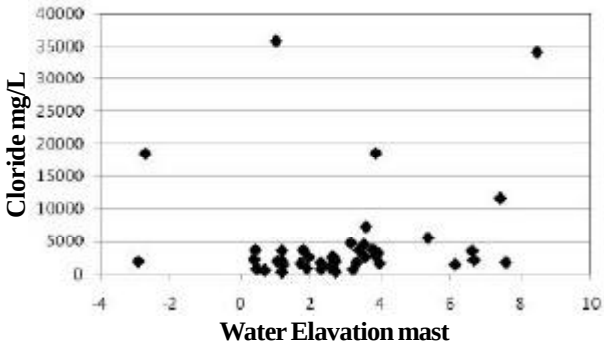

Figure 3: Data show little to no correlation between water elevation above seas level and chloride concentration a surrogate for overall salinity in this system

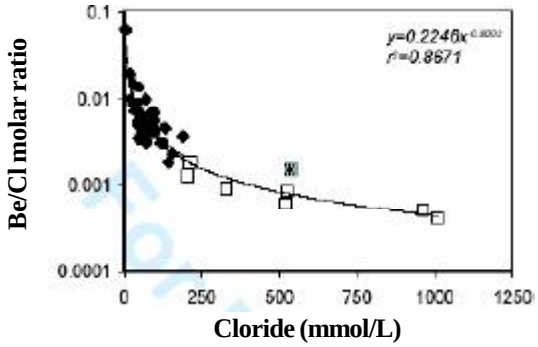

Figure 4: Graph showing chloride to bromide relations for groundwaters in El Bardaweil region. Waters with high chloride concentrations and low Cl/Br ratios are shown in open squares, remaining samples with closed diamonds and sea water composition with grey background

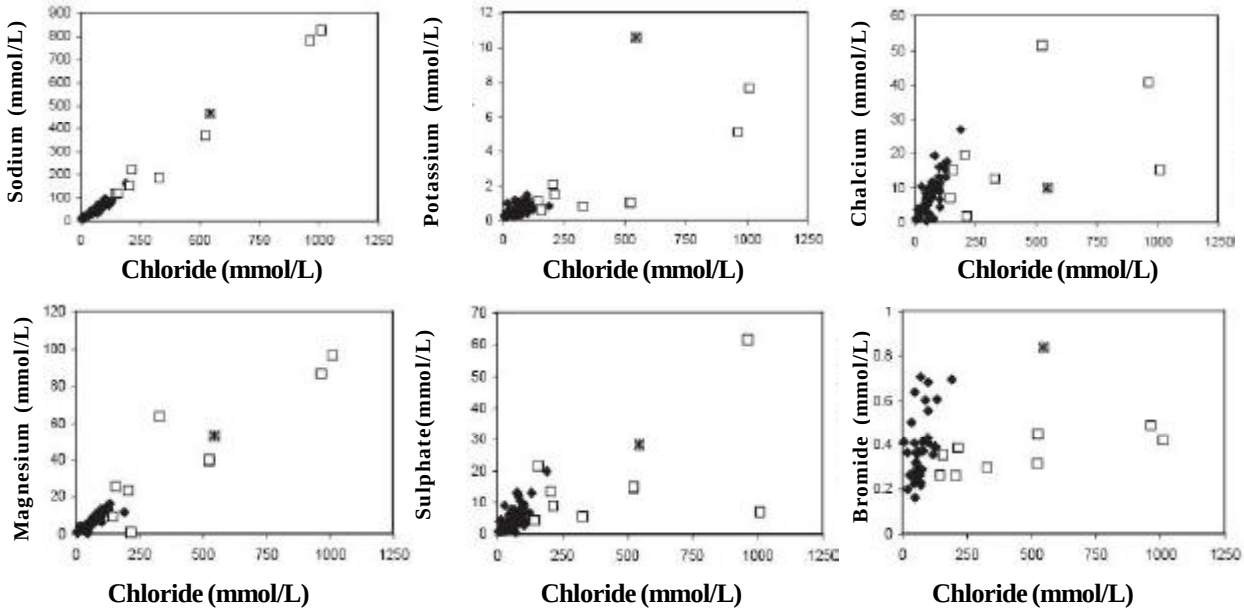

Figure 5: All graphs show Cl-rich waters with low Br/Cl ratios with open squares, remaining samples with closed diamonds and sea water composition in the grey background star symbol

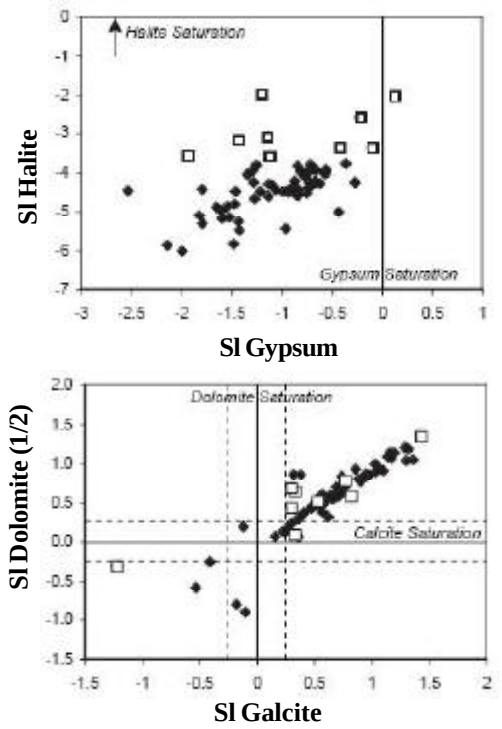

Figure 6: Saturation indices for El Bardaweil aquifer system. Groundwaters with high chloride concentration and low Br/Cl ratios are shown in open squares, remaining freshwater samples are shown in closed diamonds

TABLE 7 : Reaction path modeling results

Mineral	Mean Mineral flux (+ dissolve, - precipitate) mol/L	Stdev of Mineral flux mol/L	Mineral formula
Halite	2.74E-01	2.65E-04	NaCl
Gypsum	-3.99E+00	4.24	$CaSO_4:2H_2O$
Calcite	5.60E+00	8.34	$CaCO_3$
Dolomite	-3.51E+00	4.17	$CaMg(CO_3)_2$
Epsomite	4.01E+00	4.25	$MgSO_4:7H_2O$
Mirablite	-3.52E-02	1.50E-04	$Na_2SO_4:10H_2O$
Leonite	-1.36E-04	3.60E-04	$K_2Mg(SO_4)_2:4H_2O$

composition of seawater[15] is off the trend line connecting dilute and more concentrated waters. This result indicates that a composition different from seawater is mixing with the freshwater in this system or that there are exchange, mineral dissolution and precipitation reactions occurring. Mixing with seawater better explains magnesium and sodium chemistry but does much more poorly at explaining potassium variation with chloride in the available sample analyses. These cation results may be explainable through cation exchange between seawater and aquifer materials.

Results for anions however again show a situation that is not likely to be explained by seawater intrusion with both sulfate and bromide graphed against chloride showing that mixing between fresh and sea waters is not likely to be a good explanation of chemical concentration variability in the aquifer. Notably seawater is much more enriched in bromide than all samples in the aquifer. For sulfate, seawater is a potential component but not a reliable one as high chloride samples consistently have lower sulfate concentrations than those in seawater and the higher salinity samples do not plot on anything resembling a mixing line between the freshwater samples in the aquifer and seawater.

Saturation index results indicate several features about the chemistry of this system. The only chemicals to have positive saturation indices are calcite (or aragonite) and dolomite (Figure 6). Halite and gypsum show some variation in their saturation indices but the indices for both are never super saturated and simply go from large under saturation to only minor under saturation. Notably the saturation indices for dolomite and calcite are only under saturated in a few of the freshwater wells and all but one of the high calcite and dolomite saturation indices are in well samples with elevated chloride concentrations. Additionally, the high chloride waters contain the highest saturation indices for halite while gypsum variability in saturation index is significantly greater in high and low chloride waters. Most of the high gypsum saturation indices are found in waters that also have elevated chloride concentrations.

Reaction path modeling of either median or specific dilute water wells evolving into the chloride rich wells resulted in dissolution of halite into the freshwater to explain the composition of the more Cl rich water samples. The results for other mineral phases are not straightforward. While the average of the nine workable models, using the median of dilute and saline waters as initial and final composition, indicates precipitation of gypsum, some models show dissolution and others precipitation. In all models some dissolution of a sulfate bearing mineral is present along with the dissolution of calcite and the precipitation of dolomite. Combined, the results indicate chloride salts are dissolving along with the dissolution of calcium rich carbonates and the precipitation of magnesium rich carbonates. Sulfate model results are more ambiguous but in general indicate more sulfate dissolution than precipitation on average (TABLE 7).

DISCUSSION

Salinity source

Increases in salinity in this system appear to be due to dissolution of evaporite minerals as opposed to intrusion of seawater. This conclusion can only be drawn by relying on several lines of evidence. First, the hydraulic head of the system does not have a strong correlation to variation in total dissolved solids (Figure 3). This lack of correlation by itself is not conclusive but indicates that areas of lower hydraulic head where we might expect seawater intrusion to be most evident are not in fact the areas of highest salinity as such a model might indicate (Figure 1 and Figure 2). Second, while some dissolved species such as Mg and Na appear to be either a mixture of salt and fresh waters or of evapoconcentrated water this sort of a mixing and evaporation mechanism falls apart for SO_4 and Br and by inference from there Cl concentration (Figure 5). In particular, the low Br/Cl ratios of high Cl concentration waters (shown in Figure 3) imply that dissolution of Br-depleted evaporite minerals explains the chemical composition of the system.

Chemical evolution

The reaction path and saturation index modeling done in PHREEQC appears to support the evaporite dissolution hypothesis via several means. First of all, saturation indices for halite become much closer to one for the more Cl rich waters in the system. Second, the reaction path results consistently include halite as one of the most prominent minerals dissolving in this system. Some may view this as a result of the limited mineral assemblage used in our modeling (NaCl is the only Cl bearing salt). While certainly over simplified it was found when other chloride salts were included it simply results in dissolution of one salt and precipitation of another with the net chemical change being dissolution of halite. So in the interest of simplicity the more limited mineral assemblage results reported here were utilized.

We do not intend for our reaction path results to be a definitive result that is uncontestable but rather we use the results to indicate the sorts of minerals that must be dissolving to explain the composition we observe. They are one more piece of evidence that evaporite dissolution is the process driving the chemical evolution of El Bardaweil aquifer system.

Sabkhas and dolomite

Extensive research has shown that coastal sabkhas are one of the most important environments in the present day where dolomitization of sediments can occur. Most evidence points to interaction between sabkhas and marine water inputs through tidal pumping and subsequent geochemical reactions in which magnesium (from seawater) substitutes for calcium in aragonite and thus results in formation of dolomite in situ[3]. Existing studies of sabkhas and the formation of dolomite have focused on a specific set of chemical conditions-circum-neutral pH, sulfide reducing conditions and saturation with respect to gypsum[6,8,10,13]. Our system is not saturated with respect to gypsum (Figure 6). Additionally there is little evidence of sulfate reduction within this system considering the increasing sulfate concentrations, a lack of increase in alkalinity in the system in general and with no general correlation between decreases in gypsum saturation simultaneous to increases in dolomite saturation. Instead of the more traditional hypothesized pathway of dolomitization occurring in coastal sahbkas with full connection to seawater and tidal forces[4] here it appears that dolomitization is an ongoing process with the interaction of freshwater recharge with the Mg-rich evaporites left behind in a coastal sabkha from a previous period of land seawater interaction. Our hypothesis here is similar to research in the near coastal zone in the Coorong basin of Australia where it has been demonstrated that evaporating groundwaters are critical sites of dolomite formation[17], however more recently it has been shown that sulphate reduction is also an important process in the Coorong district of Australia[18], as indicated in this El Bardaweil system sulfate reduction does not appear to be an important process.

The evidence justifying this hypothesis is several fold. First, there is a strong positive correlation for calcite and dolomite saturation indices (SI) (Figure 6). Second, many of the SI values for dolomite are greater than one again indicating that the precipitation of dolomite is possible (Figure 6). Third, the molar ratio of Mg/Ca in this system is greater than one for 35% (25/70) of the samples collected. As stated by Margaritz et al.[9] a ratio greater than one for Mg/Ca is a fundamental precondition for dolomitization. While the ratio is often greater than one (sometimes as high as 12) there is not a specific structure of this ratio relating it to other

geochemical properties in the system (results not shown). Fourth, inverse geochemical modeling within PHREEQ indicates that dolomite precipitates in this system as water evolves from upland freshwater to lowland saline water locations (TABLE 7). This dissolution of calcite and precipitation of dolomite is the precise mechanism that is believed to occur during dolomitization of limestones[2].

Our model of how this might work is dissolution of evaporites and carbonate minerals increases alkalinity and calcium and magnesium concentrations along with the overall increase in salinity with halite dissolution. The increase in calcium and magnesium likely comes from sulfate salts and thus the source of magnesium might be epsomite or a similar mineral. With the increase in alkalinity, calcium and magnesium, the system becomes supersaturated with respect to dolomite and calcite (Figure 6). This hypothesis differs from traditional views since instead of dolomitization occurring in an organic rich reducing environment it instead occurs in a carbon poor sand aquifer system with evaporite dissolution interacting with incoming freshwater to cause dolomitization within the aquifer material. The proposed mechanism hypothesizes that dolomitization occurs due to groundwater-evaporites interaction as opposed to the more commonly hypothesized seawater intrusion mechanism. This interaction would still occur in coastal environments the cause would just be a difference in where the additional water and solutes are coming from. Instead of from the ocean the water and solutes originate on land and interact with terrestrial evaporite deposits. Our proposed mechanism needs further documentation including mineralogical analysis of sediments demonstrating the presence of dolomite.

CONCLUSIONS

Several results from this study are of particular importance. First, this near coastal aquifer system is not currently subject to seawater intrusion but rather to evaporite dissolution, a process and problem likely to be present in other recently coastal sabkha environments in arid and semiarid sea coasts around the globe. Second, the identification of dolomitization occurring in this system is important as we may have identified an alternative mechanism for dolomitization that involves the interaction of fresh groundwaters with evaporite dissolution and precipitation of dolomite. Finally, the mechanism of salinization in this region indicates that ongoing efforts to irrigate this region with Nile river water should proceed carefully and avoid areas with evaporites as much as possible due to the adverse soil and water salinization that would likely occur.

REFERENCES

[1] M.S.Andersen, N.R.Jakobsen, D.Postama; Geochimica Et Cosmochimica Acta, **69(16)**, 3979-3994 **(2005)**.

[2] S.J.Burns, J.A.McKenzie, C.Vasconcelos; Sedimentology, **47(s1)**, 49-61 **(2000)**

[3] R.Curtis, G.Evans, D.J.Kinsman, D.J.Shearman; Nature, **197**, 679-680 **(1963)**.

[4] J.I.Drever; The geochemistry of natural waters surface and groundwater environments.Upper Saddle River, NJ: Prentice Hall, **(1997)**.

[5] M.J.Fishman, L.C.Friedman; Methods for Determination of Inorganic Substances in Water and Fluvial Sediments, Washington DC: USGS, **(1989)**.

[6] E.Gavish; Sedimentology, **21**, 397-414 **(1974)**.

[7] K.Hyeong, R.M.Capuana; Geochimica et Cosmo Chimica Acta, **65(18)**, 3065-3080 **(2001)**.

[8] R.V.Lloyd, J.W.Morrison, D.N.Lumsden; Geochimica Et Cosmochimica Acta, **57**, 1071-1078 **(1993)**.

[9] M.Margaritz, L.Goldenberg, U.Kafri, A.Arad; Nature, **287(5783)**, 622-624 **(1980)**.

[10] N.F.Moreira, L.W.Walter, C.Vasconcelos, J.A.McKenzie, P.J.McCall; Geology, **32**, **(8)**, 701-704 **(2004)**.

[11] D.L.Parkhurst; User's guide to PHREEQC a computer program for speciation, reactionpath, advective-transport and inverse geochemical calculations, Washington DC: USGS, 95-4227 **(1995)**.

[12] F.H.Rainwater, L.L.Thatcher; Methods for Collection and Analysis of Water Samples, 1454 **(1968)**.

[13] W.E.Sanford, W.W.Wood; Hydrogeology Journal, **9**, 358-366 **(2001)**.

[14] K.Szramek, J.C.McIntosh, E.L.Williams, T.Kanduc, N.Ogrinc, L.M.Walter; Geochemistry, Geophysics,Geosystems, 8, 4, Q04002,doi:10.1029/2006GC001337, **(2007)**.

[15] K.K.Turekian; Oceans. Prentice-Hall, **(1968)**.

[16] A.Vengosh, B.Sherwood-Lollar; 'Salinization and Saline Environments', Environmental Geochemistry, Amstredam: Elsevier, 333-366 **(2007)**.

[17] C.C.Von der Borch, D.E.Lock, D.Schwebel; Geol., **3(5)**, 283-5 **(1975)**.

[18] D.T.Wright, D.Wacey; Sed., **52(5)**, 987-1008 **(2005)**.